N^6-methyladenosine Reader YTHDF1-induced lncRNA DLGAP1-AS2 Promotes the c-Myc Mediated Gastric Cancer Aerobic Glycolysis

Changshun Yang
Fujian Provincial Hospital
Yu Zhang
Fujian Provincial Hospital
Xuefei Cheng
Fujian Provincial Hospital
Weihua Li (doctorlinan.edu@aliyun.com)
Fujian Provincial Hospital https://orcid.org/0000-0002-0384-5194

Primary research

Keywords: N6-methyladenosine, gastric cancer, aerobic glycolysis, DLGAP1-AS2, YTHDF1.

Posted Date: September 20th, 2021

DOI: https://doi.org/10.21203/rs.3.rs-797863/v1

Abstract

Background: Emerging data has demonstrated the essential function of N^6-methyladenosine (m^6A) modification of long non-coding RNAs (lncRNAs) in human tumorigenesis. Nevertheless, the regulation of m^6A-lncRNA approach on gastric cancer (GC) tumorigenesis is unclear.

Methods: LncRNA expression profile data was derived from GEO. M^6A profile was screened using Methylated RNA immunoprecipitation sequencing (MeRIP-Seq). The metabolism assays were conducted using quantitative analysis of glucose, lactate, ATP and extracellular acidification rate (ECAR). The m^6A level of specific RNA was identified using MeRIP-qPCR. The molecular interaction was detected using RIP assay.

Results: In the findings, results showed that enhanced DLGAP1-AS2 expression was correlated with advanced pathological stage and poor prognosis. Functionally, DLGAP1-AS2 promoted the aerobic glycolysis and knockdown of DLGAP1-AS2 suppressed the tumor growth of GC cells. Mechanistically, m^6A reader YTHDF1 accelerated the enrichment of DLGAP1-AS2 in GC. Moreover, DLGAP1-AS2 interacted with YTHDF1 to integrate c-Myc mRNA, thereby enhancing the stability of c-Myc mRNA through DLGAP1-AS2/m^6A/YTHDF1/c-Myc mRNA.

Conclusions: In conclusion, our work indicates a novel m^6A-maintained lncRNA DLGAP1-AS2 in the GC aerobic glycolysis, disclosing a m^6A-reader-dependent modality regulation.

Introduction

Gastric cancer (GC) is a worldwide digestive system malignant tumor with a significant high mortality and morbidity[1,2]. In spite of the achievement on the GC therapy, including chemotherapy, radiotherapy and surgery, the overall survival rate or survival time of GC sufferers remains unimproved[3]. The reason for the lethal trait of GC is metastases and recurrence, however, the molecular mechanisms for GC progression is still poorly understood[4]. Therefore, it is significantly critical to explore the underlying mechanism of GC development, covering prognostic biomarkers, diagnostic and therapeutic targets.

Long non-coding RNAs (lncRNAs) are novel noncoding RNAs longer than 200 nucleotides length without protein-coding potential[5,6]. Over the years of research, growing number of lncRNAs are identified in the GC occurrence[7,8]. For example, lncRNA MAGI2-AS3 promotes the tumor progression through sponging miR-141/200a to overexpress ZEB1 level, highlighting an ideal biomarker for GC potential therapeutic target[9]. SNHG11 post-transcriptionally promotes oncogenic autophagy progression through aggravating ATG12 and CTNNB1 through miR-483-3p and miR-1276[10]. In summary, these findings suggest that lncRNA may function as an essential regulator in GC progression.

N^6-methyladenosine (m^6A) is the most prevalent internal modification connected with eukaryotic mRNAs fate, including mRNA metabolism, splicing, export and stability[11–13]. Besides, in various tumor

physiological events, m^{6}A participates in these tumor progression related progresses[14]. For example, major m^{6}A methyltransferase METTL3 expression elevated in GC tissue and was predictive of poor prognosis. The stability of ZMYM1 mRNA was enhanced by through METTL3 relying on reader protein HuR[15]. Wilms' tumour 1-associated protein (WTAP) highly expressed in GC cells and tissue, which indicates a poor prognosis for GC patients and correlated with a cell-related immune response[16]. Thus, these evidences support that m^{6}A modification significantly modulates the GC carcinogenesis.

Herein, we found a new evidence that lncRNA DLGAP1-AS2 was highly expressed in GC, which was correlated with poor prognosis and advanced clinical stage. Moreover, m^{6}A modified lncRNA DLGAP1-AS2 potentiated the aerobic glycolysis of GC through post-translational regulation of c-Myc mRNA stability in m^{6}A-dependent manner.

Results

DLGAP1-AS2 was an up-regulated lncRNA in GC

Using the microarray data (GSE157289), we found that numerous lncRNAs were de-regulated in the GC tissue samples (**Figure 1A**). Moreover, we found that a potential up-regulated lncRNA (DLGAP1-AS2) might be correlated with the GC carcinogenesis. In GC cell lines, expression of DLGAP1-AS2) over-expressed as comparing to the normal cell lines (**Figure 1B**). In GC samples, DLGAP1-AS2 levels significantly over-expressed as comparing to the normal adjacent tissue (**Figure 1C**). Kaplan-Meier analysis and log-rank test found that GC tissue samples with high DLGAP1-AS2 levels displayed a lower survival rate as the control cohort (**Figure 1D**). Therefore, these data revealed an up-regulated lncRNA DLGAP1-AS2 in GC.

m^{6}A-modified DLGAP1-AS2 demonstrated higher stability mediated by m^{6}A reader YTHDF1

MeRIP-Seq in GC cells revealed the m^{6}A peaks density, including 5’-UTR, coding region (CDS) and 3’-UTR (**Figure 2A**). The significant m^{6}A motif for the m^{6}A peaks was GGAC (**Figure 2B**). MeRIP-Seq demonstrated that there was a remarkable m^{6}A modification site in the 3’-UTR region of DLGAP1-AS2 (**Figure 2C**). In the exploration which m^{6}A enzyme catalyzes the m^{6}A modification on DLGAP1-AS2, we found that m^{6}A reader YTHDF1 was positively correlated to the level of DLGAP1-AS2 (**Figure 2D**). This clue indicated that m^{6}A reader YTHDF1 might regulate the fate of DLGAP1-AS2. MeRIP-qPCR showed that the enforced YTHDF1 could significantly promote the m^{6}A-installed DLGAP1-AS2 expression (**Figure 2E**). RNA stability analysis found that the enforced YTHDF1 accelerated the RNA stability of DLGAP1-AS2 in SGC7901 cells (**Figure 2F**). In summary, these findings revealed that m^{6}A-modified DLGAP1-AS2 demonstrated higher stability mediated by m^{6}A reader YTHDF1.

DLGAP1-AS2promoted the aerobic glycolysis of GC

In the functional experiments, enhanced expression or silencing of DLGAP1-AS2 was constructed in MKN45 or SGC7901 cells (**Figure 3A**). Subsequently, the biological functions of DLGAP1-AS2 on GC aerobic glycolysis were investigated. Glucose uptake analysis illustrate that enforced DLGAP1-AS2 expression promoted the glucose consumption in MKN45 cells, and knockdown of DLGAP1-AS2 repressed the glucose consumption in SGC7901 cells (**Figure 3B**). Lactate production analysis unveiled that enforced DLGAP1-AS2 expression accelerated the lactate production in MKN45 cells, and knockdown of DLGAP1-AS2 inhibited the lactate production in SGC7901 cells (**Figure 3C**). ATP quantitative analysis illustrated that enforced DLGAP1-AS2 expression facilitated the ATP production in MKN45 cells, and knockdown of DLGAP1-AS2 restrained the ATP production in SGC7901 cells (**Figure 3D**). ECAR analysis for GC glycolytic ability illustrated that enforced DLGAP1-AS2 expression promoted the extracellular acidification accumulation (**Figure 3E**), and knockdown of DLGAP1-AS2 repressed the acidification (**Figure 3F**). Moreover, the in vivo animal experiments indicated that knockdown of DLGAP1-AS2 inhibited the tumor neoplasm growth of GC cells (**Figure 3G**). In conclusion, these findings demonstrated that DLGAP1-AS2 promoted the aerobic glycolysis of GC

c-Myc acted as a target of DLGAP1-AS2

On the basis of finding that DLGAP1-AS2 regulated the aerobic glycolysis, we assumed that DLGAP1-AS2 might regulate certain key enzyme of glycolysis. In the GEPIA database, we found that c-Myc was positively correlated with DLGAP1-AS2 and YTHDF1, indicating that c-Myc might act a target of DLGAP1-AS2 (**Figure 4A**). Besides, the c-Myc levels were highly expressed in the stomach neoplasm (STAD, Stomach adenocarcinoma) (**Figure 4B**). MeRIP-Seq found that there was a m^6A site in the c-Myc mRNA, suggesting a potential regulation for DLGAP1-AS2 via m^6A-dependent manner (**Figure 4C**). Localization analysis found that DLGAP1-AS2 distribution was in accordance with the c-Myc (**Figure 4D**). The coincident cytoplasmic distribution of DLGAP1-AS2 and c-Myc indicated the potential interaction within them. In summary, these data illustrated that c-Myc acted as a target of DLGAP1-AS2.

DLGAP1-AS2promoted c-Myc mRNA stability through m^6A-YTHDF1-dependent manner

The MeRIP-Seq demonstrated that there was a m^6A modification site in the 3'-UTR of c-Myc mRNA, which was in accord with the CAGAC motif (**Figure 5A**). MeRIP-qPCR suggested us that the m^6A enrichment on c-Myc mRNA was higher in the GC cells (MKN45, GC7901) (**Figure 5B)**. Moreover, the RNA immunoprecipitation (RIP) unveiled that enhanced DLGAP1-AS2 expression promoted the c-Myc mRNA level precipitated by the anti-YTHDF1 antibody (**Figure 5B, left)**. Besides, knockdown of DLGAP1-AS2 inhibited the c-Myc mRNA level (**Figure 5B, right)**. RT-qPCR found that enhanced DLGAP1-AS2 expression amplified the c-Myc mRNA level (**Figure 5D, up)**. Moreover, the knockdown of DLGAP1-AS2 decreased the c-Myc mRNA level (**Figure 5D, down)**. RNA stability analysis found that DLGAP1-AS2 overexpression promoted the c-Myc mRNA remaining level, and the knockdown of DLGAP1-AS2 repressed the c-Myc mRNA remaining (**Figure 5E)**. In summary, these findings illustrated that DLGAP1-AS2 promoted c-Myc mRNA stability through m^6A-YTHDF1-dependent manner.

Discussion

As one of the most prominent characteristics of malignant tumors, aerobic glycolysis (also known as Warburg effect) is a complex process affected by genetic and epigenetic modifications[17,18]. For the regulation of tumorigenesis, aerobic glycolysis exerts critical roles on the progress of tumor cell energy metabolism, providing the main energy supplement. In the current study, we demonstrated that DLGAP1-AS2 expression was increased in GC tissues and cell lines. Furthermore, a high DLGAP1-AS2 expression implied a poor prognosis for GC.

Here, we found that DLGAP1-AS2 expression was significantly up-regulated in the GC and moreover promoted the glucose uptake, lactate production and ATP generation. Our results reflect this possibility that DLGAP1-AS2 may act as an energy metabolism-related oncogene in GC. Accumulating evidences have illustrated that lncRNA plays critical roles in cancer aerobic glycolysis. For instance, the over-expressed LINC00242 promotes the GC proliferation and aerobic glycolysis in vitro and relieves the tumorigenesis in vivo through directly targeting G6PD[19]. LINC01391 overexpression hampers the proliferation, invasion and aerobic glycolysis in *vitro* and tumor growth in *vivo* of GC, while LINC01391 knockdown shows the opposite results[20]. Overexpressed DLX6-AS1 in GC significantly promotes cell viability and colony formation, and then regulates aerobic glycolysis by targeting phosphoinositide-dependent protein kinase 1 (PDK1)[21]. These results consistently emphasized the regulation of lncRNAs for GC aerobic glycolysis.

To further validate the biological function of lncRNA on GC, we utilized the MeRIP-Seq and found that there was a potential m^{6}A site in the 3'-UTR of DLGAP1-AS2, suggesting the m^{6}A modification for DLGAP1-AS2. The specific m^{6}A modification on DLGAP1-AS2 could significantly modulate its fate. In our research, we found that the m^{6}A reader YTHDF1 could specifically bind with the m^{6}A site on the DLGAP1-AS2. Besides, YTHDF1 could assist the stability increasing for DLGAP1-AS2. DLGAP1-AS2, on the other hand, connected with its downstream targets through m^{6}A binding. Mechanistically, we found that m^{6}A-modified DLGAP1-AS2 functions through a YTHDF1-involved m^{6}A mechanism. DLGAP1-AS2 integrated with c-Myc mRNA via the m^{6}A-mediated combination, constructing a DLGAP1-AS2/m^{6}A/YTHDF1/c-Myc mRNA axis.

On this basis of m^{6}A-DLGAP1-AS2, we realize the importance that m^{6}A-modified lncRNA provides an important regulatory pattern for human cancer. For instance, lncRNA LINRIS is upregulated in colorectal cancer, and LINRIS knockdown attenuates the degradation of IGF2BP2 and especially MYC-mediated glycolysis[22]. For another example, m^{6}A is highly enriched on the lncRNA THOR transcripts, including GAACA, GGACU and UGACU motifs. Besides, m^{6}A-modified lncRNA THOR regulates the cancer cells' proliferation via an m^{6}A-reader-dependent manner[23]. In colorectal cancer, m^{6}A-induced lncRNA RP11 triggers the progression and metastasis via post-translational Zeb1 upregulation through RP11/hnRNPA2B1/mRNA complex[24]. These results consistently demonstrated the m^{6}A-lncRNA interaction regulation for human cancer.

In summary, our findings in this study revealed that DLGAP1-AS2 promoted the tumorigenesis of GC through m^6A/YTHDF1/c-Myc mRNA axis, thus triggering c-Myc mRNA stability and accelerating the aerobic glycolysis of GC cells. These m^6A-dependent RNA-protein interactions could maintain the oncogenic characteristic of lncRNA DLGAP1-AS2. DLGAP1-AS2 may serve as potential target in the GC treatment.

Materials And Methods

Patient tissues specimens collection

A total of 50 GC tissue samples in the cohort, which were formalin-fixed and paraffin-embedded, were recruited between January 2016 and December 2018 from patients who had underwent operation in Fujian Provincial Hospital. All samples were staged according to the criteria of the 7^{th} Edition of the AJCC Cancer Staging Manual (Stomach, 2010)[25]. This study was approved by the Fujian Provincial Hospital Ethics Review Committee. Informed consent was written by each patient before the study.

Cell culture

GC cell lines (AGS, BGC823, MKN45, SGC7901) and the immortalized human gastric epithelial cell line (GES-1) were purchased from the Cell Bank of the Chinese Academy of Sciences. The cells were maintained in RPMI-1640 medium supplemented with 10% fetal bovine serum (HyClone, Logan, UT, USA) and antibiotics at 37 °C under 5% CO_2.

Transfection vector construction

For the stable silencing of DLGAP1-AS2, lentivirus vector pLKD-U6-shRNA-EF1a-LUC-F2A-Puro-DLGAP1-AS2 (Obio Technology, shanghai, China) or control vectors were packaged and transfected into SGC7901 cells. Cell were grown in 1 μg/ml puromycin (Invitrogen) to select the stable transfected cells. Moreover, for the overexpression of DLGAP1-AS2, the cDNA of DLGAP1-AS2 was PCR-amplified ad then sub-cloned into pcDNA 3.1 vector (Invitrogen, Carlsbad, Calif, USA). The efficiency of silencing or overexpression was subsequently quantified by qRT-PCR. The siRNAs and their controls (si-NC) were provided by GenePharma (Shanghai, China) and transfected using Lipofectamine 2000 (Invitrogen) when 70 % confluent growth.

Quantitative real-time PCR (qRT-PCR)

Total RNA from GC tissues or cell lines was extracted by TRIzol Reagent (Invitrogen, CA, USA). For the concentration and purity of RNA, RNA was detected with ultraviolet spectrophotometer using 260 nm and 280 nm. The real-time PCR was performed using SYBR Premix Ex Taq (Takara) on the 7900 Real-time PCR System. Reverse transcription was performed using PrimerScript RT Reagent Kit (TaKaRa, Kyoto, Japan). Fast SYBR green master mix (Life Technologies) applied to perform qRT-PCR. The relative expression was calculated using the $2^{-\triangle\triangle CT}$ method. The β-actin acted as the internal mRNA control. The primer sequences were displayed in **Table S1**.

Western blot assay

The procedure details were conducted according to previous study. Proteins from transfected GC cells were extracted using RIPA buffer (Beyotime, China) and authenticated using BCA Kit (Pierce, Rockford, IL, USA). Protein was resolved using the SDS-PAGE Electrophoresis System and then transferred to PVDF membranes (Millipore, USA). Specific primary antibodies were incubated at 4 °C overnight. β-actin was the internal reference.

Methylated RNA immunoprecipitation sequencing (MeRIP-Seq)

MeRIP-seq with data analysis was performed as previously described[26]. In brief, total RNA was extracted using Trizol (Invitrogen) and then purified using Gen Elute mRNA Miniprep Kit (Sigma-Aldrich). RNA was fragmented by RNA fragmentation kit (Ambion, Austin, TX, USA) and immunoprecipitated with Protein A beads the mixture (Thermo Fisher) containing anti-m^6A antibody (Synaptic Systems). The immunoprecipitated RNA was eluted following the manufacturer's instructions. Library was constructed using purified RNA fragments from m^6A MeRIP and sequenced with Illumina Nextseq500.

Methylated RNA immunoprecipitation (MeRIP) qPCR

All the specific manipulations were performed according to the protocol of Magna MeRIP™ m^6A Kit (Merck Millipore). In brief, total RNAs were isolated from SGC7901 or MKN45 cells and chemically fragmented into 100-300 nt. Fragmented fragments were incubated with m^6A antibody for immunoprecipitation. The enrichment of m^6A containing mRNA was sent for quantitative RT-PCR. The RT-qPCR primers were listed in **Table S1**.

Quantitative analysis of glucose, lactate and ATP

The glucose uptake was quantificationally detected using Glucose Uptake Assay Kit (Fluorometric, Abcam, ab136956). The lactate production was quantificationally detected using Lactate Colorimetric/Fluorometric Assay Kit (BioVision, K607–100). The ATP generation was quantificationally detected using ATP Assay Kit (Beyotime, S0026).

Measurement of extracellular acidification rate (ECAR)

ECAR was analyzed using Seahorse XFe96 analyzer (Seahorse Bioscience, Agilent) as previously described. Briefly, knockdown and overexpression of DLGAP1-AS2 transfected cells (1×10^4 cells/well) seeded into 96-well XF cell culture microplate. Medium (pH 7.4) was sequentially added with 10 mM glucose, 1 mM glutamine, 50 mM 2-DG and 1 μM oligomycin. ECAR was shown in mpH/min and measured using an XF96 analyzer.

Actinomycin D assay

SGC7901 cells were seeded in 6-well plates (2×10^5 cells/well). 24 hours later, cells were exposed to Actinomycin D (Act D, 2 μg/ml, Sigma) and harvested at indicated time point. The RNA remaining level was analyzed using qRT-PCR and normalized to mock group (0 hour).

RNA immunoprecipitation (RIP) assay

RIP assay was performed using EZ-Magna RIP™ RNA-Binding Protein Immunoprecipitation Kit (Millipore, USA) according to manufacturer's protocol. Specific antibodies (anti-YTHDF1, Abcam) was conjugated with magnetic beads and then dissolved in RIP buffer. Approximate 90% confluence, cells were lysed using complete RIP lysis buffer (100 μl) containing protease inhibitor and RNase Inhibitor (Millipore). Mouse anti-IgG antibody (Cell Signaling Technology, USA) acted as negative control. Then, total RNA was retrieved and the relative expression was detected by qRT-PCR analysis.

Localization of DLGAP1-AS2

Probes were obtained from Genepharma (Shanghai, China). Fluorescence in situ hybridization (FISH) was performed using fluorescent in situ hybridization kit according to the manufacturer's protocols (Genepharma). Cy3-labeled probe for DLGAP1-AS2 and FAM-labeled probe for c-Myc were used for localization of DLGAP1-AS2 and c-Myc in GC cells. Nuclei was stained with 4,6-diamidino-2-phenylindole (DAPI) and images were obtained using confocal microscope (Olympus).

Animal models in *vivo*

Approximately 2×10^6 GC cells (SGC7901), transfected with sh-DLGAP1-AS2 or controls, were suspended in 100 μl PBS and then injected into flank of male BALB/c nude mice (5-week old). In the following observation, tumor size was recorded by vernier caliper. At the indicated time, mice were anesthetized and sacrificed for tumors neoplasm acquisition. All animal assays were performed in the light of institutional Fujian Provincial Hospital Animal Ethics Committee guidelines.

Statistical analysis

The data was expressed as mean ± S.D (standard deviation). All results were conducted using SPSS Statistics software (Armonk, NY, USA) or GraphPad prism 7.0 (La Jolla, CA, USA). Difference within groups was calculated using One-way ANOVA test, non-parametric Mann-Whitney test and student's t-test. Overall survival rate was calculated using Kaplan-Meier analysis and log-rank test. *$P \leq 0.05$ or **$P \leq 0.01$ was considered statistically significant.

Declarations

Ethics approval and consent to participate

This study was approved by the Fujian Provincial Hospital Ethics Review Committee. Informed consent was written by each patient before the study.

Consent for publication

All authors agree with the publication.

Availability of data and materials

Not applicable.

Competing interests

All authors declare no conflicts of interest

Funding

Not applicable.

Authors' contributions

Changshun Yang and Yu Zhang performed the assays and were responsible for the writing. Xuefei Cheng was responsible for the statistic. Weihua Li was responsible for the funding and design.

Acknowledgements

Not applicable.

References

1. Machlowska J, Baj J, Sitarz M, Maciejewski R, Sitarz R. (2020) Gastric Cancer: Epidemiology, Risk Factors, Classification, Genomic Characteristics and Treatment Strategies. Int J Mol Sci 21(11).
2. Sexton RE, Al Hallak MN, Diab M, Azmi AS. (2020) Gastric cancer: a comprehensive review of current and future treatment strategies. Cancer Metastasis Rev 39(4):1179-1203.
3. Smyth EC, Nilsson M, Grabsch HI, van Grieken NC, Lordick F. (2020) Gastric cancer. Lancet 396(10251):635-648.
4. Tang T, Zhang L, Li C, Zhou T. (2020) Gastric and adrenal metastasis from breast cancer: Case report and review of literature. Medicine (Baltimore) 99(3):e18812.
5. Gil N, Ulitsky I. (2020) Regulation of gene expression by cis-acting long non-coding RNAs. Nat Rev Genet 21(2):102-117.
6. Jiang G, Su Z, Liang X, Huang Y, Lan Z, Jiang X. (2020) Long non-coding RNAs in prostate tumorigenesis and therapy (Review). Mol Clin Oncol 13(6):76.
7. Joshi M, Rajender S. (2020) Long non-coding RNAs (lncRNAs) in spermatogenesis and male infertility. Reprod Biol Endocrinol 18(1):103.
8. Tornesello ML, Faraonio R, Buonaguro L, Annunziata C, Starita N, Cerasuolo A, Pezzuto F, Tornesello AL, Buonaguro FM. (2020) The Role of microRNAs, Long Non-coding RNAs, and Circular RNAs in

Cervical Cancer. Front Oncol 10:150.

9. Li D, Wang J, Zhang M, Hu X, She J, Qiu X, Zhang X, Xu L, Liu Y, Qin S. (2020) LncRNA MAGI2-AS3 Is Regulated by BRD4 and Promotes Gastric Cancer Progression via Maintaining ZEB1 Overexpression by Sponging miR-141/200a. Mol Ther Nucleic Acids 19:109-123.
10. Wu Q, Ma J, Wei J, Meng W, Wang Y, Shi M. (2021) lncRNA SNHG11 Promotes Gastric Cancer Progression by Activating the Wnt/β-Catenin Pathway and Oncogenic Autophagy. Mol Ther 29(3):1258-1278.
11. Huang H, Weng H, Chen J. (2020) m(6)A Modification in Coding and Non-coding RNAs: Roles and Therapeutic Implications in Cancer. Cancer Cell 37(3):270-288.
12. Ma Z, Ji J. (2020) N6-methyladenosine (m6A) RNA modification in cancer stem cells. Stem Cells.
13. Zhu ZM, Huo FC, Pei DS. (2020) Function and evolution of RNA N6-methyladenosine modification. Int J Biol Sci 16(11):1929-1940.
14. Wang YN, Yu CY, Jin HZ. (2020) RNA N(6)-Methyladenosine Modifications and the Immune Response. J Immunol Res 2020:6327614.
15. Yue B, Song C, Yang L, Cui R, Cheng X, Zhang Z, Zhao G. (2019) METTL3-mediated N6-methyladenosine modification is critical for epithelial-mesenchymal transition and metastasis of gastric cancer. Mol Cancer 18(1):142.
16. Li H, Su Q, Li B, Lan L, Wang C, Li W, Wang G, Chen W, He Y, Zhang C. (2020) High expression of WTAP leads to poor prognosis of gastric cancer by influencing tumour-associated T lymphocyte infiltration. J Cell Mol Med 24(8):4452-4465.
17. Huang S, Guo Y, Li Z, Zhang Y, Zhou T, You W, Pan K, Li W. (2020) A systematic review of metabolomic profiling of gastric cancer and esophageal cancer. Cancer Biol Med 17(1):181-198.
18. Yuan LW, Yamashita H, Seto Y. (2016) Glucose metabolism in gastric cancer: The cutting-edge. World J Gastroenterol 22(6):2046-59.
19. Deng P, Li K, Gu F, Zhang T, Zhao W, Sun M, Hou B. (2021) LINC00242/miR-1-3p/G6PD axis regulates Warburg effect and affects gastric cancer proliferation and apoptosis. Mol Med 27(1):9.
20. Qian C, Xu Z, Chen L, Wang Y, Yao J. (2020) Long noncoding RNA LINC01391 restrained gastric cancer aerobic glycolysis and tumorigenesis via targeting miR-12116/CMTM2 axis. J Cancer 11(21):6264-6276.
21. Qian Y, Song W, Wu X, Hou G, Wang H, Hang X, Xia T. (2021) DLX6 Antisense RNA 1 Modulates Glucose Metabolism and Cell Growth in Gastric Cancer by Targeting microRNA-4290. Dig Dis Sci 66(2):460-473.
22. Wang Y, Lu JH, Wu QN, Jin Y, Wang DS, Chen YX, Liu J, Luo XJ, Meng Q, Pu HY*, et al*. (2019) LncRNA LINRIS stabilizes IGF2BP2 and promotes the aerobic glycolysis in colorectal cancer. Mol Cancer 18(1):174.
23. Liu H, Xu Y, Yao B, Sui T, Lai L, Li Z. (2020) A novel N6-methyladenosine (m6A)-dependent fate decision for the lncRNA THOR. Cell Death Dis 11(8):613.

24. Wu Y, Yang X, Chen Z, Tian L, Jiang G, Chen F, Li J, An P, Lu L, Luo N*, et al*. (2019) m(6)A-induced lncRNA RP11 triggers the dissemination of colorectal cancer cells via upregulation of Zeb1. Mol Cancer 18(1):87.
25. Washington K. (2010) 7th edition of the AJCC cancer staging manual: stomach. Ann Surg Oncol 17(12):3077-9.
26. Yang F, Jin H, Que B, Chao Y, Zhang H, Ying X, Zhou Z, Yuan Z, Su J, Wu B*, et al*. (2019) Dynamic m(6)A mRNA methylation reveals the role of METTL3-m(6)A-CDCP1 signaling axis in chemical carcinogenesis. Oncogene 38(24):4755-4772.

Tables

Table 1. DLGAP1-AS2 expression and GC patients' clinicopathological characteristic.

		50	DLGAP1-AS2		p-value
			Low	High	
Age	< 55	29	17	12	0.726
	≥ 55	21	8	13	
Gender	Male	26	14	12	0.197
	Female	24	11	13	
TNM stage	I/II	13	7	6	0.001*
	III/IV	37	18	19	
Lymph node metastasis	Yes	23	12	11	0.319
	No	27	13	14	
Tumor differentiation	Well	6	3	3	0.417
	Moderate	13	7	6	
	Poor	31	15	16	
Distant metastasis	Yes	17	7	10	0.367
	No	33	18	15	

Well: Well-differentiated adenocarcinoma; Moderate, moderately differentiated adenocarcinoma; Poor, poorly differentiated adenocarcinoma; TNM, tumor-node-metastasis. *P < 0.05 represents statistical differences.

Figures

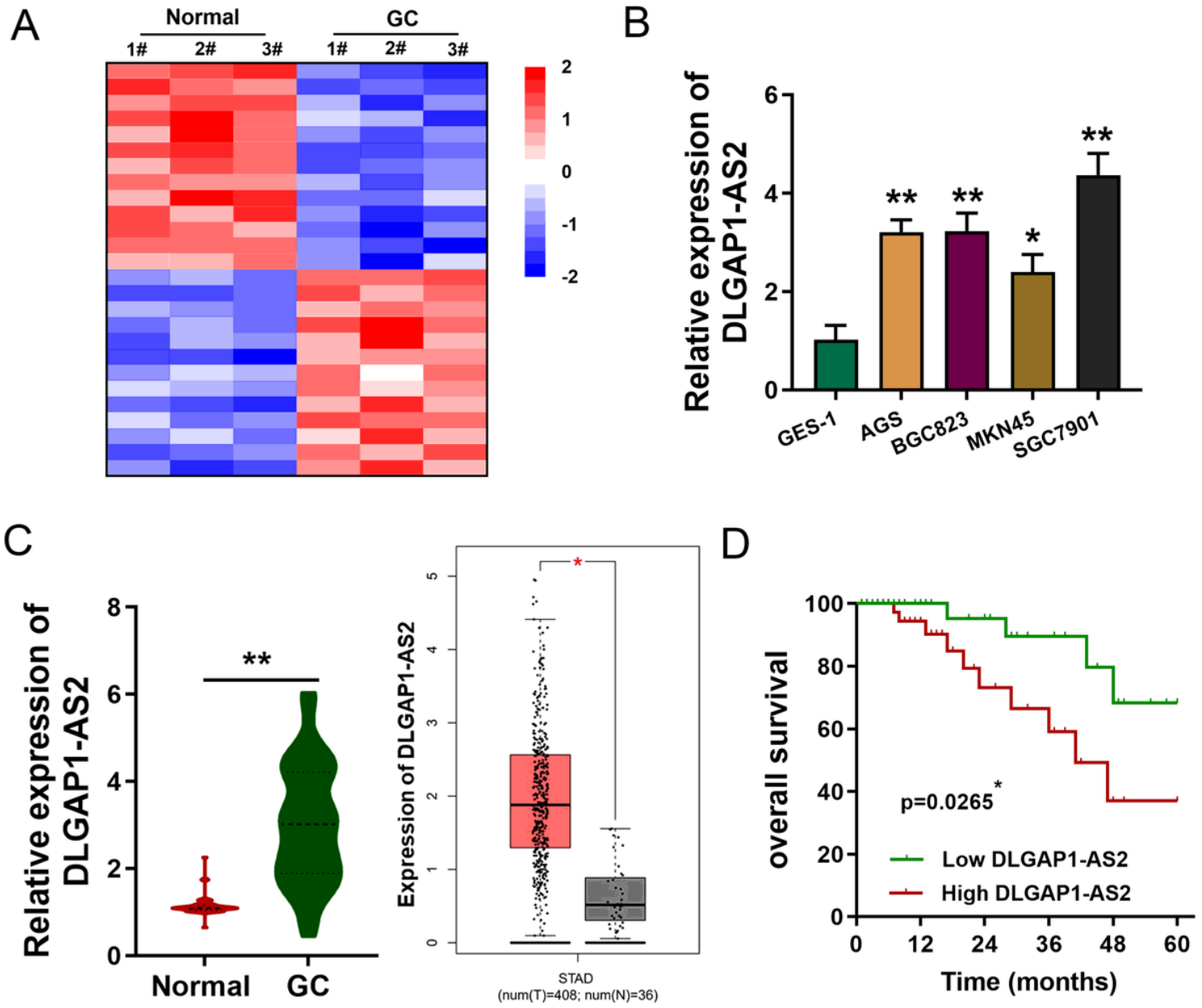

Figure 1

DLGAP1-AS2 was an up-regulated lncRNA in GC. (A) Based on the lncRNA microarray data (GSE157289), heatmap demonstrated the numerous de-regulated lncRNAs in the GC tissue as comparing to normal tissue. (B) In GC and normal cell lines cell lines, expression of DLGAP1-AS2 was detected using RT-qPCR. (C) In GC samples, DLGAP1-AS2 level was detected using RT-qPCR as comparing to the normal adjacent tissue. (D) Survival rate analysis showed the lower survival rate of GC patients with high DLGAP1-AS2 levels, while the higher survival rate of GC patients with low DLGAP1-AS2 levels. Data were expressed as mean ± SD. **p < 0.01; *p < 0.05.

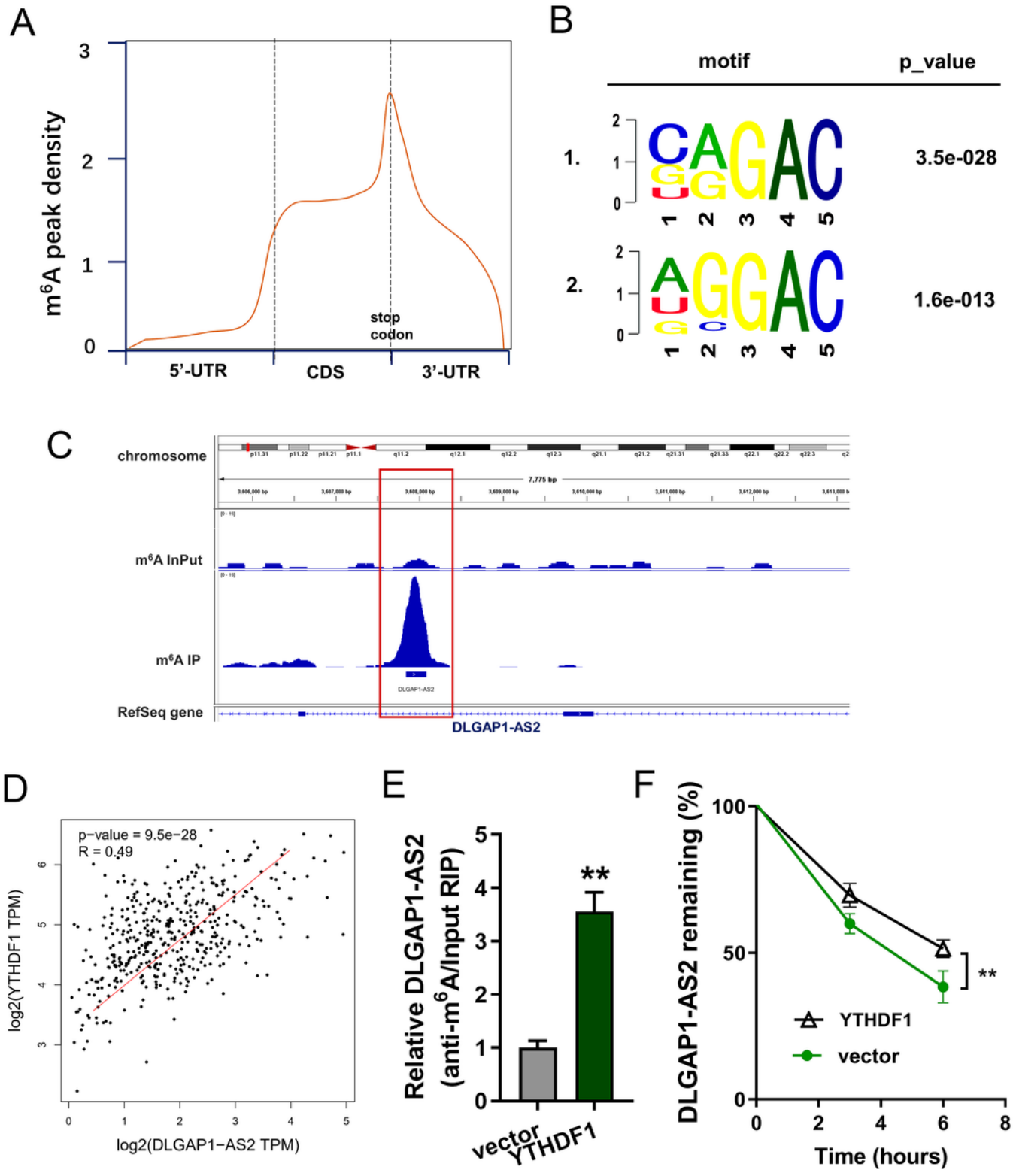

Figure 2

m6A-modified DLGAP1-AS2 demonstrated higher stability. (A) MeRIP-Seq revealed the m6A peaks density in GC cells, including 5'-UTR, coding region (CDS) and 3'-UTR. (B) The significant m6A motif for the m6A peaks was GGAC. (C) MeRIP-Seq showed that there was a remarkable m6A modification site in the 3'-UTR region of DLGAP1-AS2. (D) GEPIA dataset revealed the positive correlation within YTHDF1 and DLGAP1-AS2 in STAD (Stomach adenocarcinoma, http://gepia.cancer-pku.cn/). (E) MeRIP-qPCR showed the m6A-

installed DLGAP1-AS2 expression in SGC7901 cells precipitated by anti-YTHDF1 antibody. (F) RNA stability analysis revealed the RNA remaining of DLGAP1-AS2 in SGC7901 cells adminstered by Act D (actinomycin D, 1 μg/m). LncRNA DLGAP1-AS2 was determined by qRT-PCR assay. **p < 0.01.

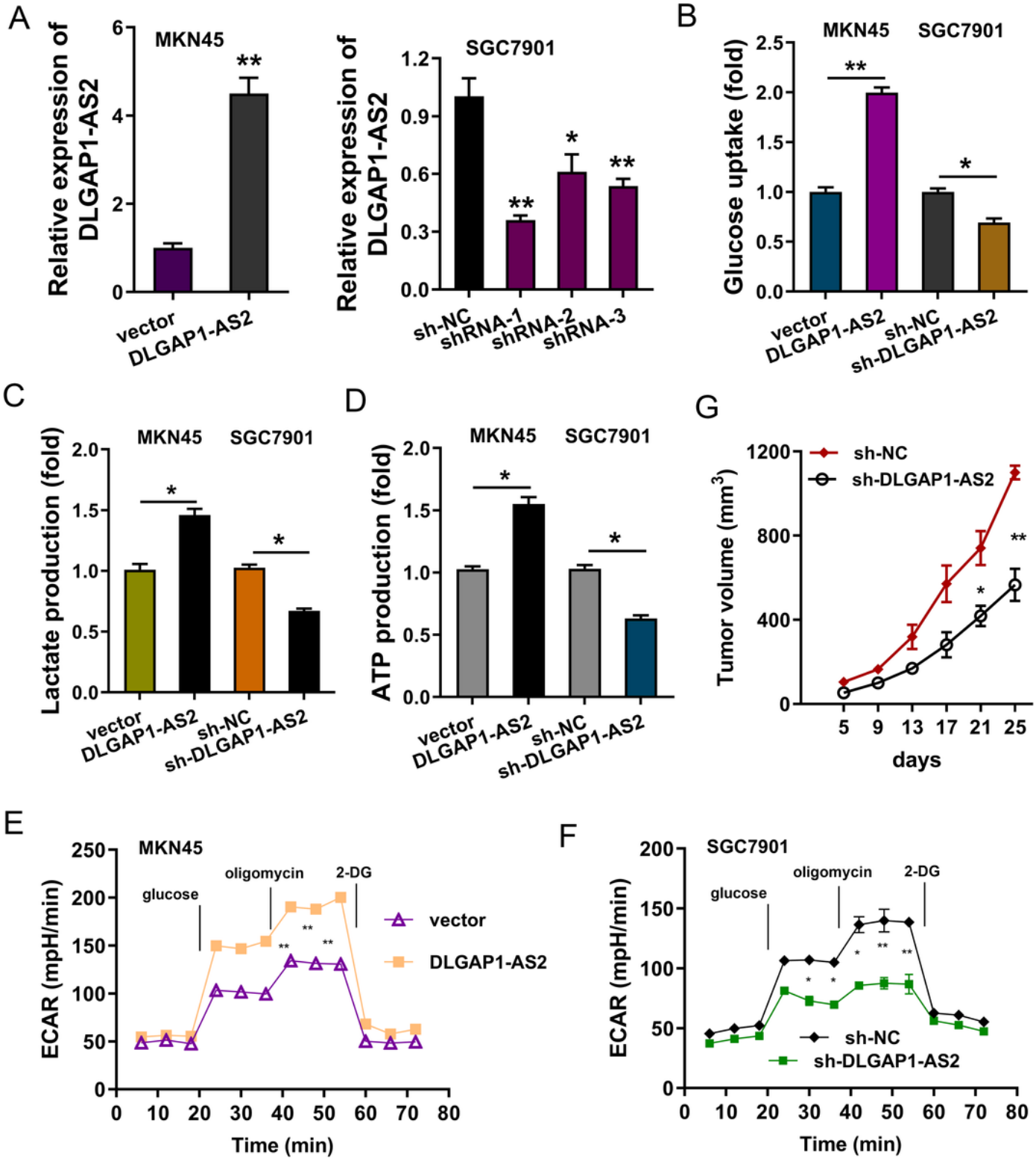

Figure 3

DLGAP1-AS2 promoted the aerobic glycolysis of GC. (A) Detection of DLGAP1-AS2 levels by qRT-PCR in GC cell lines (MKN45, SGC7901) respectively transfected with DLGAP1-AS2 overexpression plasmids or

lentivirus shRNA. (B) Glucose uptake quantity was quantificationally detected using glucose uptake kit in MKN45 and SGC7901 cells. (C) Lactate production was quantificationally detected using lactate analysis kit. (D) ATP quantitative analysis was performed in MKN45 or SGC7901 cells. (E, F) The glycolysis levels of MKN45 and SGC7901 was detected using a seahorse analyzer. (G) In vivo animal experiments were performed to test the tumor neoplasm growth of GC cells (SGC7901) transfected with DLGAP1-AS2 silencing (sh-DLGAP1-AS2). The data were presented as the mean ± SD of three independent experiments. *P < 0.05, **P < 0.01.

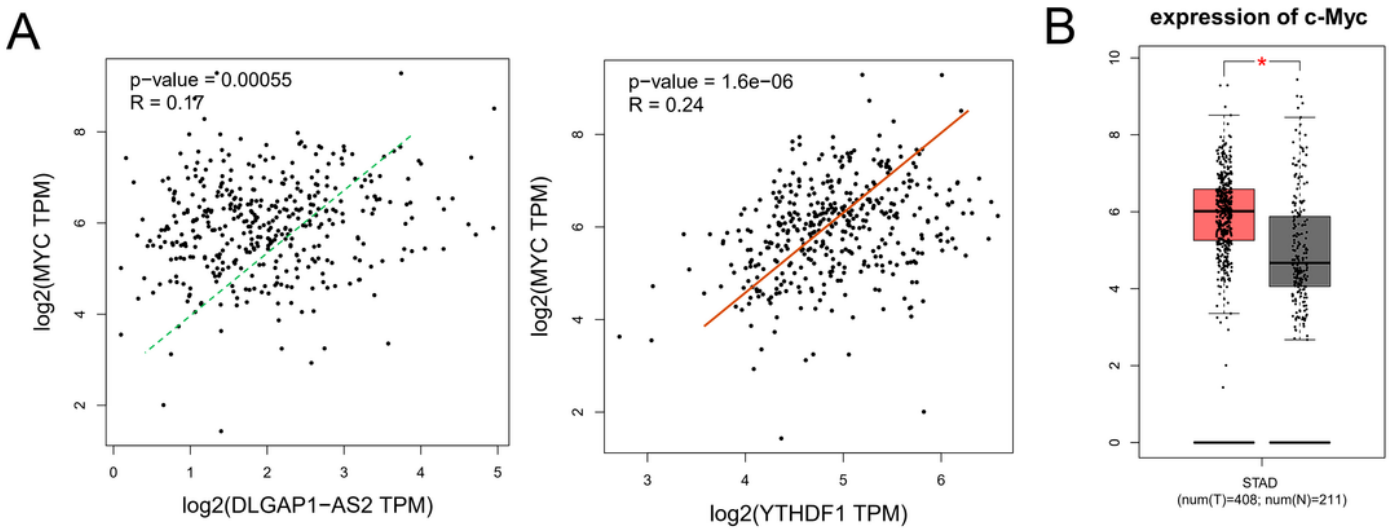

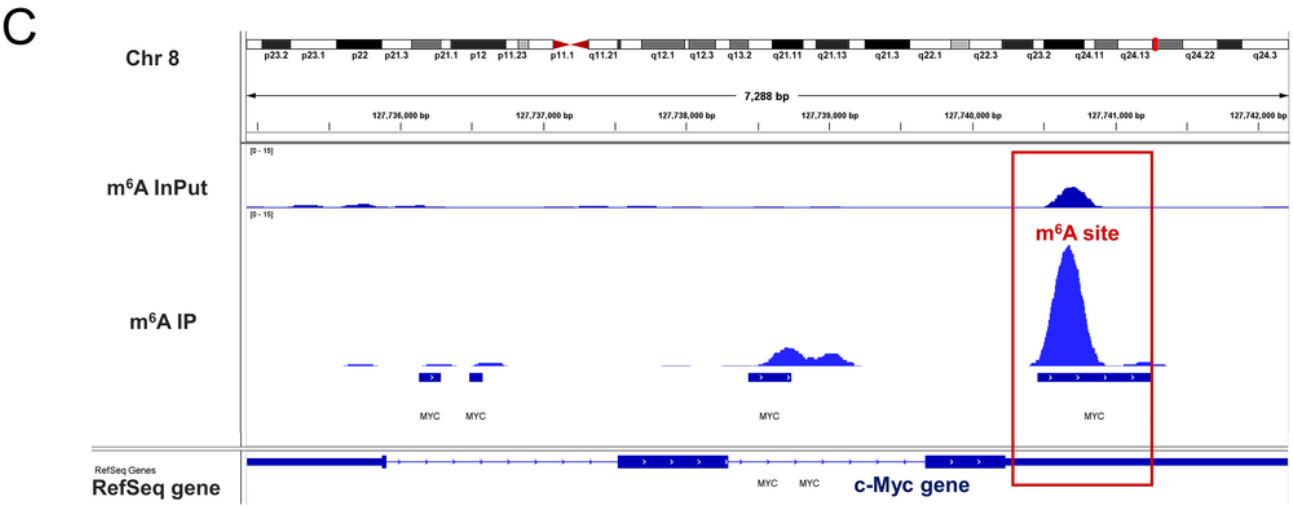

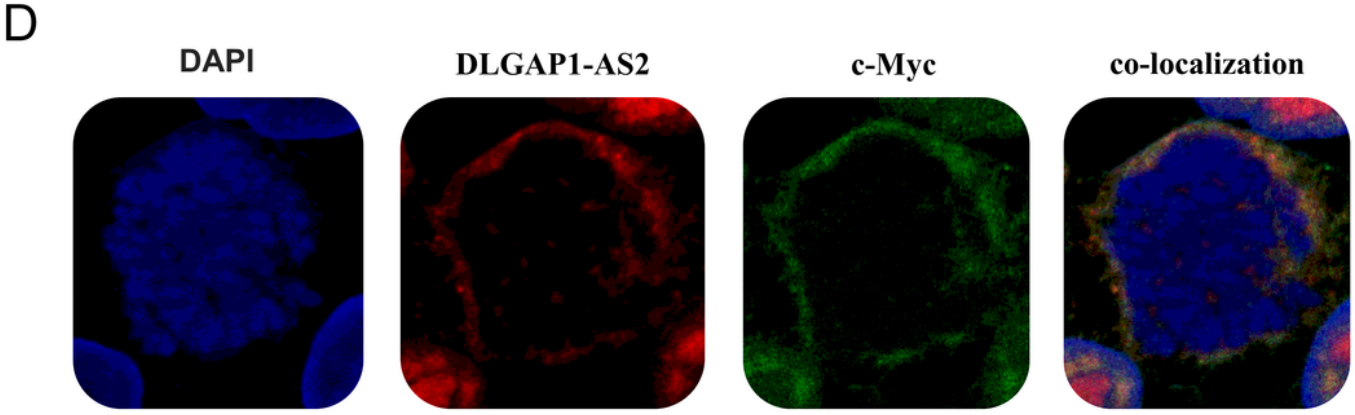

Figure 4

c-Myc acted as a target of DLGAP1-AS2. (A) GEPIA database demonstrated the positive correlation within c-Myc and DLGAP1-AS2, or c-Myc with YTHDF1 ($p<0.001$). (B) TCGA database illustrated the high-expression of c-Myc in STAD (Stomach adenocarcinoma, www.tcga.org/). (C) IGV viewer showed the m6A site in the c-Myc mRNA based on MeRIP-Seq data. (D) Co-localization analysis using fluorescence in situ hybridization (FISH) displayed the distribution of DLGAP1-AS2 and c-Myc in SGC7901 cells.

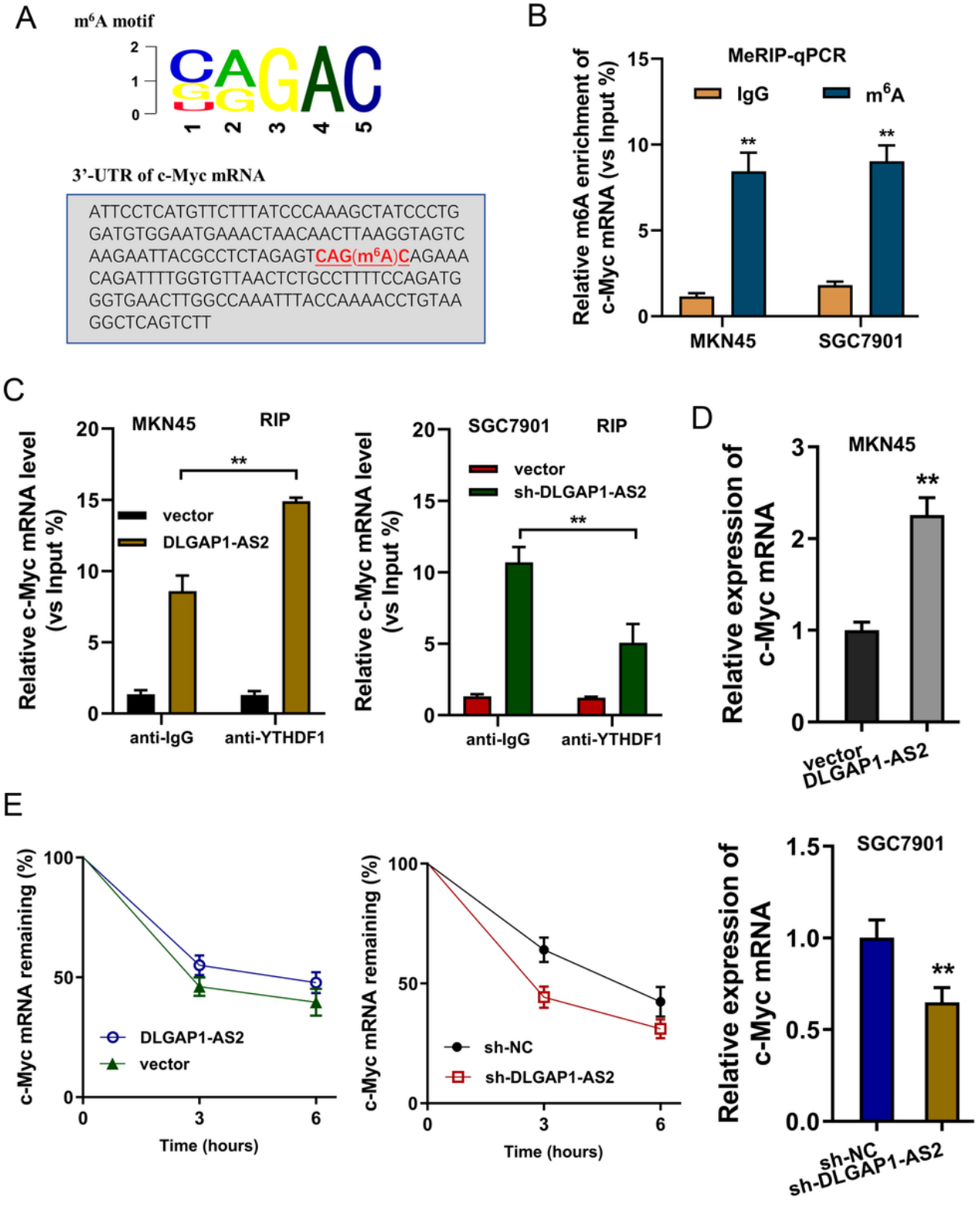

Figure 5

DLGAP1-AS2 promoted c-Myc mRNA stability through m6A-YTHDF1-dependent manner. (A) An m6A modification site in the 3'-UTR of c-Myc mRNA was discovered by MeRIP-Seq. The appropriate motif is CAGAC motif. (B) MeRIP-qPCR detected the m6A enrichment on c-Myc mRNA in GC cells (MKN45, GC7901) using m6A antibody and IgG control. (C) RNA immunoprecipitation (RIP) assays unveiled the c-Myc mRNA level precipitated by the anti-YTHDF1 antibody in in GC cells (MKN45, GC7901) transfected with DLGAP1-AS2 overexpression (DLGAP1-AS2) and knockdown (sh-DLGAP1-AS2). (D) RT-qPCR detected the c-Myc mRNA level in GC cells (MKN45, GC7901) transfected with DLGAP1-AS2 overexpression and knockdown. (E) The levels of c-Myc expression in DLGAP1-AS2-overexpressing (DLGAP1-AS2), DLGAP1-AS2 knockdown (sh-DLGAP1-AS2) and their corresponding control were detected by qRT-PCR. GC cells (MKN45, SGC7901) transfected GC cells treated with actinomycin D (2 μg/mL). **P < 0.01 vs vector control.

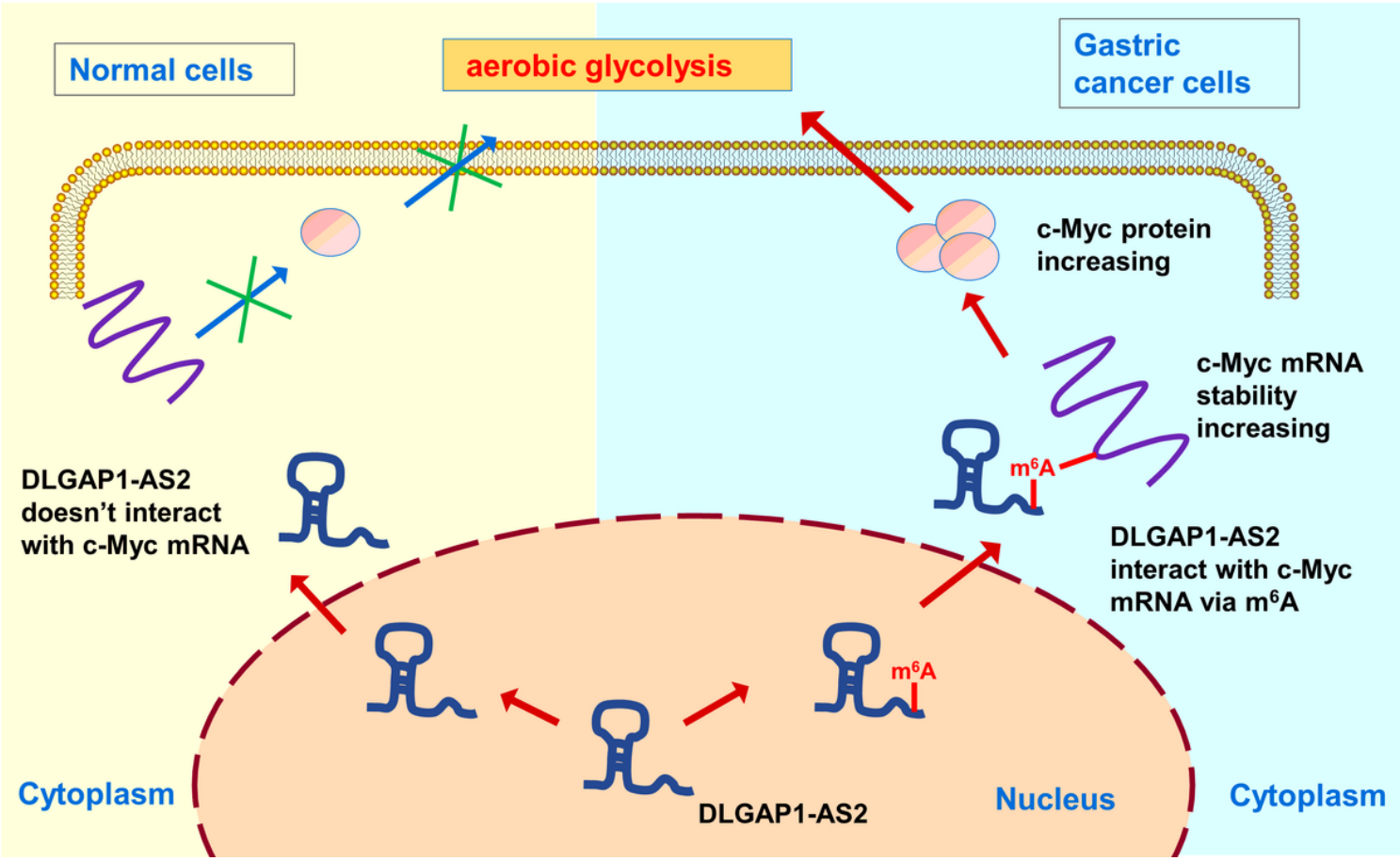

Figure 6

m6A/DLGAP1-AS2/YTHDF1/c-Myc axis promotes the aerobic glycolysis of GC.